Desalination and Water Treatment
www.deswater.com

doi: 10.1080/19443994.2015.1085912

57 (2016) 17637–17645
August

Taylor & Francis
Taylor & Francis Group

Effect of hydrophilic $Cu_3(BTC)_2$ additives on the performance of PVDF membranes for water flux improvement

Ki Yong Jee, Jae Sung Kim, Jinsoo Kim, Yong Taek Lee*

Department of Chemical Engineering, Kyung Hee University, 1 Seocheon-dong, Yongin, Gyeonggi-do 446-701, Korea, Tel. +82 31 201 2973; Fax: +82 31 204 8114; emails: ky330@khu.ac.kr (K.Y. Jee), pgwtk@khu.ac.kr (J.S. Kim), Tel. +82 31 201 2492; Fax: +82 31 204 8114; email: jkim21@khu.ac.kr (J. Kim), Tel. +82 31 201 2577; Fax: +82 31 204 8114; email: yongtlee@khu.ac.kr (Y.T. Lee)

Received 31 December 2014; Accepted 18 August 2015

ABSTRACT

In this study, a polyvinylidene fluoride (PVDF) membrane for water treatment was modified by dispersing hydrophilic metal–organic framework (MOF) particles, namely $Cu_3(BTC)_2$ and acidified $Cu_3(BTC)_2$, in a PVDF solution. The effects of the $Cu_3(BTC)_2$ and acidified $Cu_3(BTC)_2$ additives on the PVDF membranes were investigated in terms of hydrophilicity of the membrane surface and the water flux through the membrane. The PVDF membranes modified with hydrophilic MOF particles demonstrate improved water flux and maintain similar rejection values due to their improved hydrophilicity. Water fluxes of $Cu_3(BTC)_2$ and acidified $Cu_3(BTC)_2$ added membranes were 295.66 and 558 LMH which were 47 and 72.3% higher than those of the pure PVDF membrane, respectively. Acidified $Cu_3(BTC)_2$ was more stable and well immobilized in the PVDF membrane as no leaching of the metallic element was observed during the water permeation.

Keywords: Phase inversion method; PVDF membrane; MOF; $Cu_3(BTC)_2$

1. Introduction

Polyvinylidene fluoride (PVDF) has received a lot of attention as a membrane material due to its outstanding properties, such as excellent mechanical strength, thermal stability, chemical resistance, and high hydrophobicity, compared to other commercialized polymeric materials [1–3]. PVDF membranes have been used in membrane contractors and membrane distillation, as well as in microfiltration and ultrafiltration processes [1,4,5].

In recent years, many researchers have extensively investigated the modification of PVDF membranes to improve membrane performance. The addition of inorganic particles into polymer dope solutions has become an attractive method for the fabrication of polymeric membranes. Inorganic particles, such as TiO_2, Al_2O_3, ZrO_2, and SiO_2, have been incorporated into PVDF membranes [6–9]. The presence of these dispersed inorganic particles in the membrane matrix improves the membrane performance by enhancing the hydrophilicity, fouling resistance, and mass transfer in the membrane process.

Metal–organic frameworks (MOFs) have garnered attention as an attractive alternative to inorganic filler particles in polymer matrices to improve the properties of pure polymeric membranes, especially for gas separation applications. However, there are few

*Corresponding author.

reports on MOF-based, mixed-matrix membranes for water treatment. MOFs are a new class of microporous materials consisting of small, metal-containing clusters connected three-dimensionally by polyfunctional organic ligands [10]. MOF particles may be an attractive alternative to inorganic particles as additives in polymer membranes. Although many research groups have investigated dispersing MOF particles into polymer matrix membranes for the separation of gasses and binary mixtures [11–13], there has been no report on the addition of MOF particles to polymeric membranes for use in water treatment. As for using MOFs for water treatment applications, the hydrophilic properties of MOF allow it to be dissolved in water. Therefore, modified MOFs must be immobilized within the membranes in order to be useful.

Recent studies have shown that surface modification (e.g. chemical or physical modifications such as plasma treatment) can increase the dispersing properties of inorganic particles [14,15]. Chemical modification, especially using an acid treatment, is one of the simplest and most inexpensive methods to enhance the properties. Inorganic particles with oxygen defects show stronger activity and better hydrophilic capabilities.

In this study, $Cu_3(BTC)_2$ particles, a class of hydrophilic MOF species, were incorporated into PVDF membranes to improve the water permeation flux. In addition, MOF-incorporated PVDF membranes were investigated with $Cu_3(BTC)_2$ particles that had undergone surface modification via acidification to improve the hydrophilicity of the membranes as well as the immobilization of $Cu_3(BTC)_2$ particles in the PVDF membranes. The prepared membranes were analyzed by field emission scanning electron microscopy (FE-SEM), X-ray photoelectron spectroscopy (XPS), and contact angle analysis. The membrane performance was confirmed by a pure water permeation experiment, and a rejection test was performed with a poly(ethylene oxide) (PEO) solution.

2. Experimental

2.1. Materials

PVDF (Solef 1015/1001) was obtained from Solvay Korea Co. Ltd, 1-methyl-2-pyrrolidone (NMP, 99.5%), ethanol, and sulfuric acid (H_2SO_4) were purchased from Aldrich Chemical Co. Non woven polyester fabrics (AWA Paper Mfg. Co. Ltd) were used as the support material for preparing the membrane. Copper(II) nitrate hydrate [$(Cu(NO_3)_2{\cdot}3H_2O$, 98%], benzene-1,3,5-tricarboxylic acid (BTC, 95%), and poly (ethylene oxide) (PEO, MW 300,000) were obtained from Sigma-Aldrich Co.

2.2. Preparation of MOF particles

In 48 mL of deionized (DI) water, 3.5 g of copper (II) nitrate hydrate was dissolved. To this solution, 1.68 g of benzene-1,3,5-tricarboxylic acid dissolved in 48 mL of ethanol was added and mixed for 30 min. The mixed precursor solution was placed in an autoclave, followed by solvothermal treatment at 120˚C for 6 h, and allowed to cool naturally to room temperature [16]. The resulting solution, which contained $Cu_3(BTC)_2$ crystals, was dried in an oven. These $Cu_3(BTC)_2$ particles are referred to as MOFs. A part of the solution was treated with H_2SO_4 at pH 3 for 4 h at room temperature, followed by filtering and drying. The acidified $Cu_3(BTC)_2$ particles are denoted as acid-MOFs.

2.3. Preparation of PVDF membranes

The dope solution for the PVDF membrane was prepared by dissolving PVDF (16 wt%) in NMP (84 wt%). The mixture was agitated in a reaction flask under a nitrogen atmosphere at 60˚C for 24 h to obtain a homogeneous solution. The casting polymer solution was then held at 50˚C for 24 h to remove air bubbles. Then, PVDF membranes were prepared by the phase inversion technique through immersion in the polymer solution. The polymer solution was cast on the nonwoven polyester fabric with an initial thickness of 200 μm and subjected to evaporation in air for 10 s. This was immediately followed by immersion in DI water at 25˚C for 10 min. The membranes were rinsed in DI water at 80˚C for 1 h and extracted in a second DI water bath at room temperature for 24 h.

To study the effect of MOF and acid-MOF additives, 0.25 wt% MOF or acid-MOF particles were added into the dope solution of the PVDF membranes. The resulting membranes are denoted as PVDF/MOF and PVDF/acid-MOF membranes, respectively.

2.4. Characterization

X-ray diffraction (XRD) patterns of the $Cu_3(BTC)_2$ particles were collected with a M18XHF-SRA diffractometer (Mac Science) equipped with a Cu Kα radiation source ($\lambda = 1.54056$ Å). XPS was employed to analyze the chemical bonding of the MOF particles and the membranes using an Auto Probe CP Research System (Thermo Microscope Inc., USA). The cross-sections of the membranes were examined using a FE-SEM (Carl Zeiss Model LEOSUPRA 55, Germany). Energy dispersive X-ray (EDX, Carl Zeiss Model LEOSUPRA 55, Germany) dot mapping was performed to monitor the inter dispersion of $Cu_3(BTC)_2$ particles in

the membrane matrix. The hydrophilicity of the membrane was measured using contact angle analysis.

2.5. Membrane performance

The membrane performance of the prepared membranes was measured using the pure water flux and rejection tests. The permeability of the membrane was measured using the dead-end method with a pressure of 1.0 kg/cm^2 for 30 min at room temperature and the effective membrane area was 25.6 cm^2. A solution of pure water and 1,000 ppm PEO solution were tested as feeds, respectively. The pure water flux through the membrane was calculated using the following equation:

$$J = \frac{V}{At} \quad (1)$$

where V is the volume of the permeate (L), A is the membrane surface area (m^2), and t is the permeation time (h). The pure water flux data were averaged after measuring a minimum of three membrane samples.

Rejection of the membrane is defined by Eq. (2) [17]:

$$\text{Rejection } (\%) = \frac{C_f - C_p}{C_f} \times 100 \quad (2)$$

where C_f and C_p are the concentrations of the feed solution and permeate, respectively. The C_f and C_p were measured with total organic carbon (TOC) (TOC-Vcsn, Shimadzu, Japan). Cu leaching from the membranes was investigated from the permeated water using the ICP-OES instrument (Direct Reading Echelle ICP, LEEMAN).

3. Results and discussion

3.1. Characterization of MOF particles

XRD patterns for the $Cu_3(BTC)_2$ particles and acidified $Cu_3(BTC)_2$ particles are shown in Fig. 1. All samples showed good crystallinity. Both XRD patterns are in good agreement with the single-crystal data of $Cu_3(BTC)_2$ reported by Kim et al. [18], confirming the phase structure of $Cu_3(BTC)_2$. It was also observed that the intensity of the acid-MOF sample decreased due to the surface modification of the $Cu_3(BTC)_2$ crystals.

XPS was carried out on the MOF and acid-MOF samples. The main peaks observed in the survey scan are C1s, O1s, and Cu $2p_{3/2}$ peaks centered at 284.5, 531.1, and 934.14 eV, respectively [18–21]. After acidification of the MOF sample, the Cu $2p_{3/2}$ signature showed different characteristics. The MOF sample

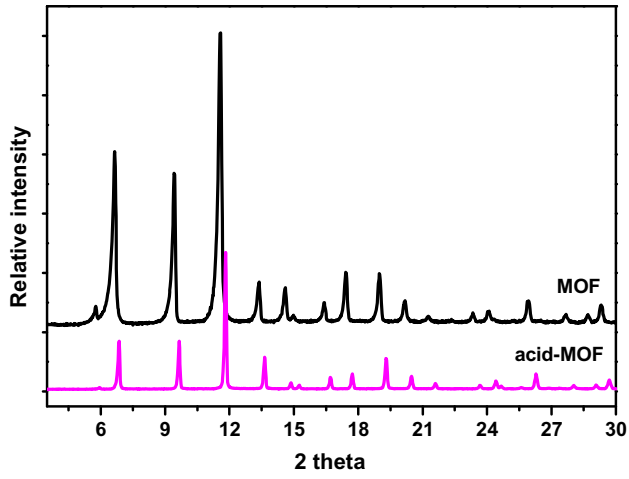

Fig. 1. XRD patterns MOF and acid-MOF particles.

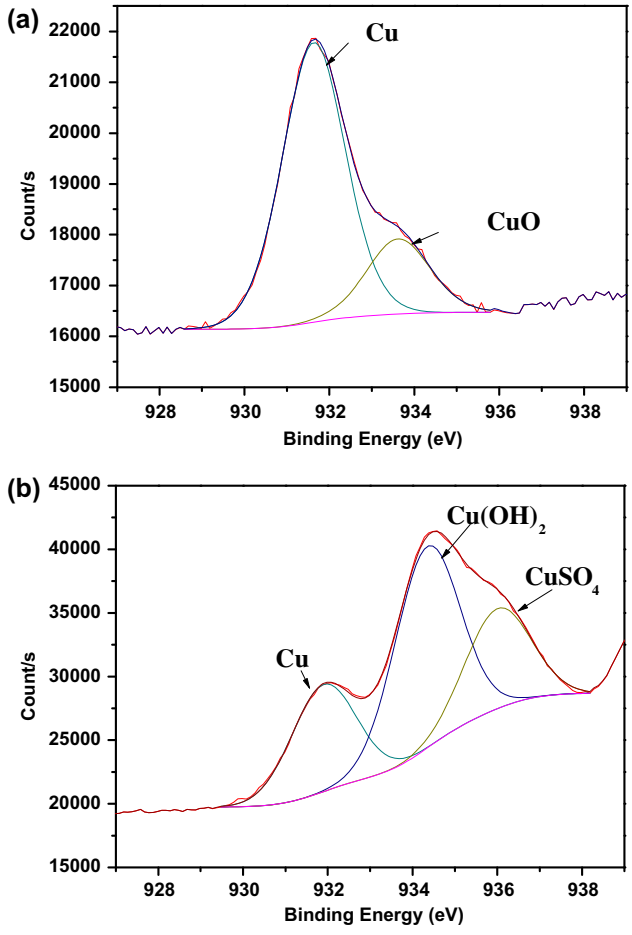

Fig. 2. XPS spectra of Cu $2p_{3/2}$ peak: (a) MOF particles and (b) acid-MOF particles.

showed only peaks of Cu at 931.63 eV (0.86%) and CuO at 933.62 eV (0.23%). Alternatively, the acid-MOF sample showed additional peaks of $Cu(OH)_2$ at 934.4 eV (2.84%) and $CuSO_4$ at 936 eV (1.41%) [22,23], in addition to the Cu and CuO peaks (Fig. 2). This difference suggests effective surface modification of the MOF samples by acidification with sulfuric acid.

3.2. Characterization of membranes

3.2.1. FE-SEM and EDX analysis

Fig. 3(a)–(c) shows the surface image of the PVDF, PVDF/MOF, and PVDF/acid-MOF membranes. All membranes have same surface structure. From the results shown, it is evident that there is no big change in the membrane morphology after adding 0.25 wt% of MOF and acid-MOF. MOF and acid-MOF particles were dispersed not only on the membrane surface but also on all the membrane pores [6].

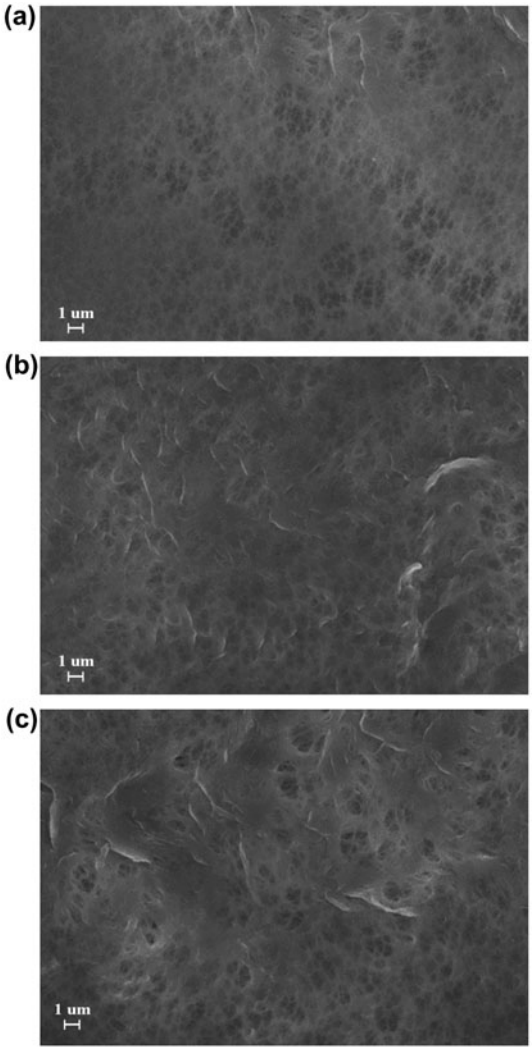

Fig. 3. Surface images of membranes; (a) PVDF membrane, (b) PVDF/MOF membrane, and (c) PVDF/acid-MOF membrane.

Fig. 4 shows the cross-sectional image of the virgin PVDF membrane prepared by the phase inversion process. A homogeneous PVDF solution is initially demixed into two liquid phases via the exchange of the solvent and the non-solvent. The phase with the higher polymer concentration forms the solid membrane, while the phase with the lower polymer concentration forms the pores of the membrane [24]. Therefore, the PVDF membrane exhibits a typical asymmetric structure with many macrovoids near the top surface due to liquid–liquid demixing. By controlling the initial stage of the phase inversion, the membrane morphology can be controlled.

The effect of the hydrophilic additives (MOF and acid-MOF particles) on the membrane morphology was investigated. Fig. 5(a)–(d) shows the cross-sectional views and EDX dot mappings (Cu) of the PVDF/MOF and PVDF/acid-MOF membranes. The EDX dot mapping results suggest that the MOF particles are uniformly distributed throughout the PVDF membranes. Although both membranes maintained the same finger-like structure as the PVDF membrane, the macrovoids became larger after the addition of the hydrophilic additives. These results are in good agreement with the findings of Fontananova et al. [24]. They reported that hydrophilic additives work as non-solvents, reducing the thermodynamic miscibility of the casting solution, and inducing an enhancement of the liquid–liquid phase separation. Therefore, systems with a rapid phase inversion rate tend to form larger macrovoids with finger-like structures.

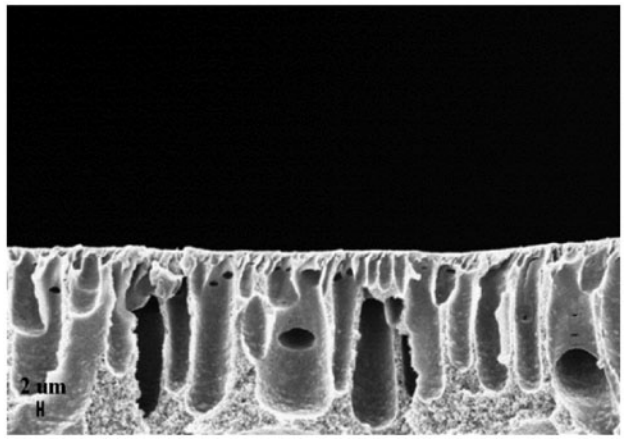

Fig. 4. Cross-sectional view of virgin PVDF membrane.

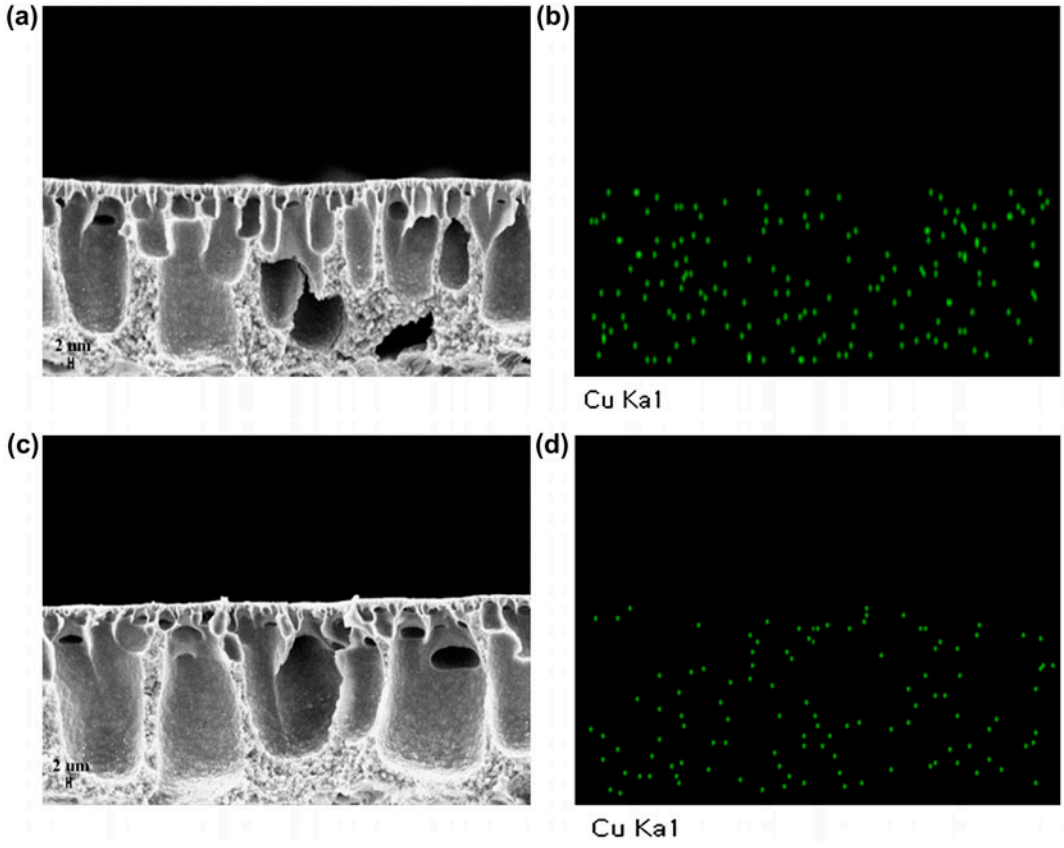

Fig. 5. Cross-sectional views (a, c) and EDX dot mappings (Cu) (b, d) of modified PVDF membranes: (a, b) PVDF/MOF membrane and (c, d) PVDF/acid-MOF membrane.

3.2.2. Contact angle analysis

In general, the hydrophilicity of membranes can be determined by the comparison of their contact angle values. Fig. 6 shows the measured contact angles for the PVDF membranes, the PVDF/MOF membrane, and the PVDF/acid-MOF membrane. The contact angle of the PVDF membrane was 78.8˚. Because of the hydrophilic properties of the MOF and acid-MOF additives, the contact angles of PVDF/MOF and PVDF/acid-MOF membranes decreased to 69.2˚ and 64˚, respectively, indicating an improved hydrophilicity. The PVDF/acid-MOF membrane showed the lowest contact angle due to the presence of more hydrophilic hydroxyl groups at the surface of the acid-MOF, which were produced through the acid treatment (see Fig. 2).

Usually, there are three major factors that affect the decay rate of a contact angle: the hydrophilicity of the membrane surface, the pore size, and the wettability of the internal pore channels [25]. In our study, the hydrophilicity of the membrane surface with the MOF additive is the main factor that causes changes in the

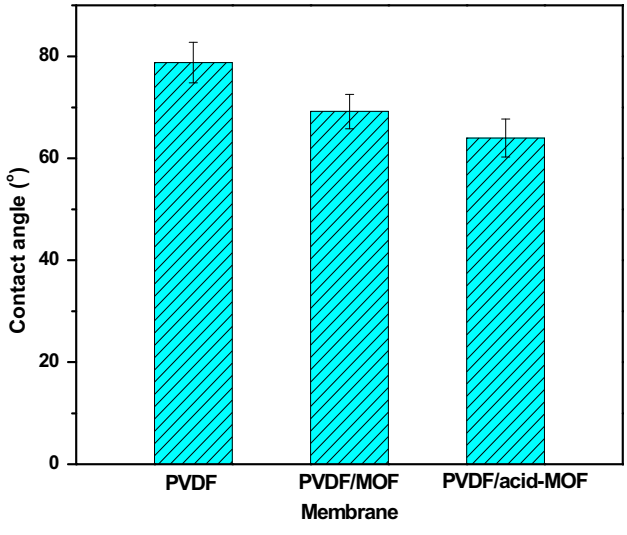

Fig. 6. Contact angle of different PVDF membranes: (a) PVDF membrane, (b) PVDF/MOF membrane, and (c) PVDF/acid-MOF membrane.

contact angle. As a result, both MOF-containing membranes have a higher hydrophilicity than the virgin PVDF membrane surface.

3.2.3. XPS analysis

The PVDF membrane is compared with the PVDF/MOF membrane and the PVDF/acid-MOF membrane in Figs. 7–9. In the case of the PVDF membrane, the C 1s core-level spectrum can be curve fitted with five peak components for C–C(285 eV, 24.24%), C–F(289.4 eV, 19.37%), C–H(283.5 eV, 10%), C–CF_2(286.8 eV, 3.68%), and $(CF_2)_n$(291.8 eV, 0.59%) for the Fig. 7 [26–28]. The C 1s peak of the PVDF/MOF membrane shows five well-resolved peaks, similar to the PVDF membrane, which correspond to C–C, C–F, C–H, C–CF_2, and $(CF_2)_n$ groups (Fig. 8(a)). The O 1s peaks show CuO(531.5 eV, 4.77%) and C–O(533.6 eV, 0.26%) (Fig. 8(b)), while the Cu $2p_{3/2}$ peak(932.5 eV, 0.05%) can be attributed to Cu (Fig. 8(c)) [22,29].

XPS of the PVDF/acid-MOF membrane showed the following features: two main C 1s peaks (285 eV, 23.31% and 289.5 eV, 19.29%) corresponding to C–C and CF, respectively. There were also four small C 1s components (283.51 eV, 6.35%; 286.07 eV, 3.25%; and 291.7 eV, 0.62%) due to C–H, C–CF_2, and $(CF_2)_n$; signs of chemical modification were also observed [C–O (287.22 eV, 2.78%)]. Alternatively, the C–H peak decreased as a result of the sulfuric acid exposure in MOF (Fig. 9(a)); The O 1s and Cu $2p_{3/2}$ peaks were similar with CuO, C–O, and Cu. However, new components were found in the fine structure of the O 1s peak (531.4 eV, 3.11%; for OH^- (Fig. 9(b)), and the Cu $2p_{3/2}$ peak (934.4 eV, 0.04%; for CuO, respectively (Fig. 9(c)) [23,26,30,31].

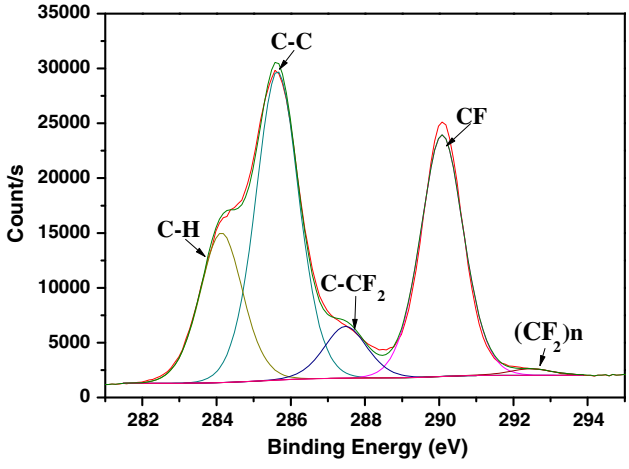

Fig. 7. The C 1s curve fitting of XPS spectrum data of the virgin PVDF membrane.

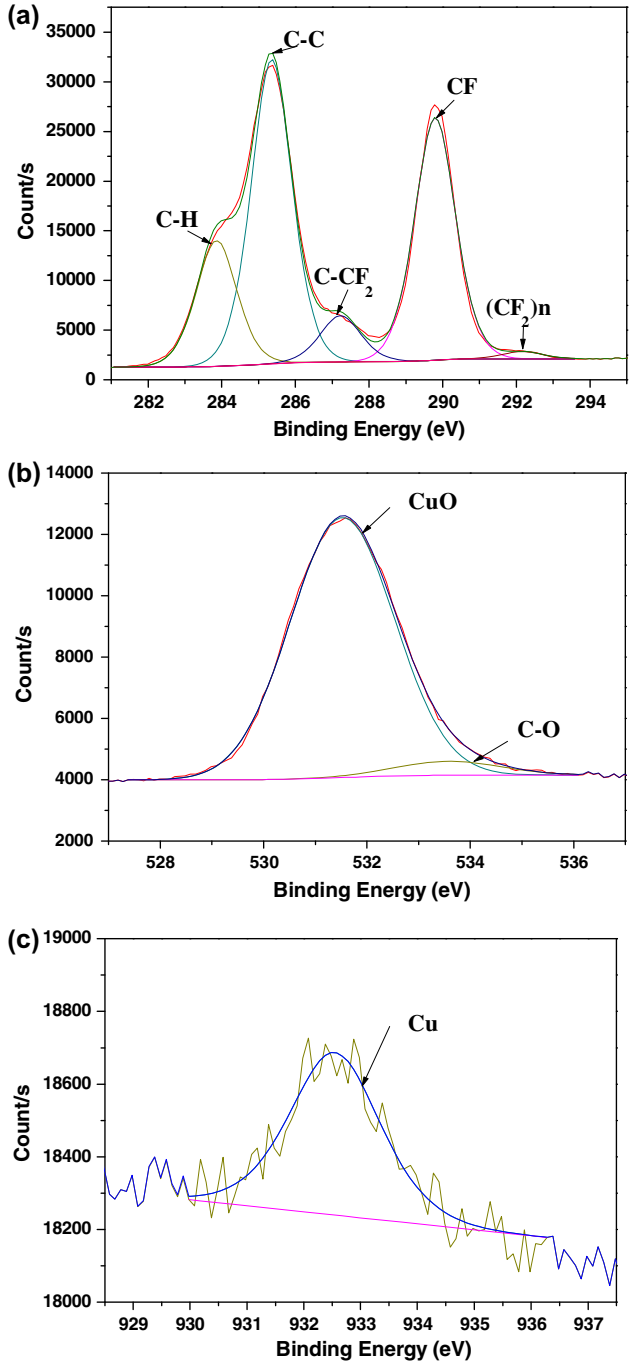

Fig. 8. Evolution of XPS spectra of PVDF/MOF membrane: (a) C 1s, (b) O 1s, and (c) Cu 2p3.

3.3. Membrane performance

The water permeability test of the prepared membranes was carried out using cross-flow filtration with pure water. The results of the permeability through the PVDF, PVDF/MOF, and PVDF/acid-MOF membranes are shown in Fig. 10. The pure water flux

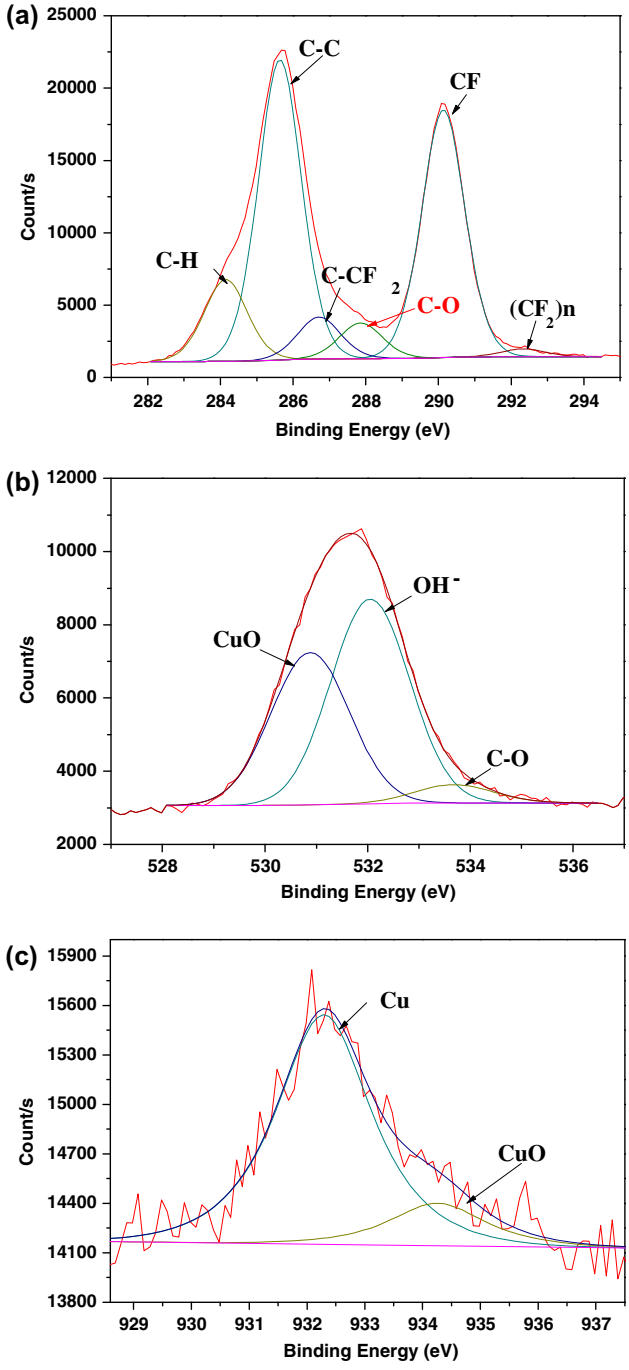

Fig. 9. Evolution of XPS spectra of PVDF/acid-MOF membrane: (a) C 1s, (b) O 1s, and (c) Cu 2p3.

through the PVDF membrane showed 154.7 LMH. However, when the hydrophilic MOF and acid-MOF particles were added into the PVDF membranes, the pure water fluxes of the membranes increased to 299.7 and 558 LMH, respectively. In general, the water permeation flux is determined by the morphology and hydrophilicity of the membranes. The rapid increase

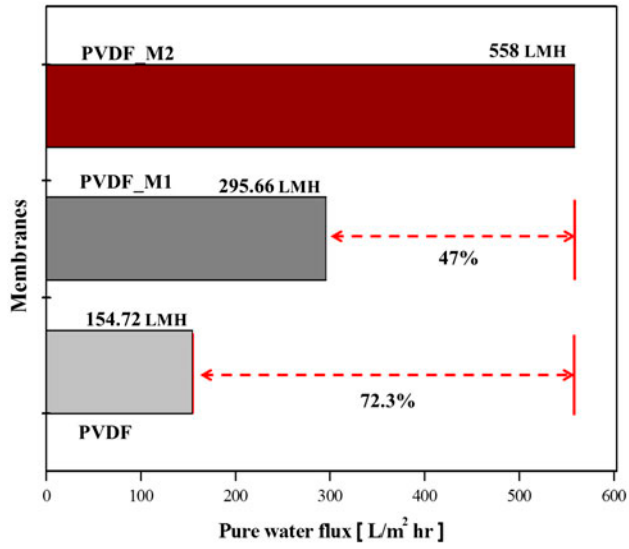

Fig. 10. Pure water flux data through PVDF, PVDF/MOF, and PVDF/acid-MOF membranes.

in the water permeation flux through the PVDF/MOF and PVDF/acid-MOF membranes is attributed to the presence of larger macrovoids [8], shown in Fig. 5, as well as the improved hydrophilicity (confirmed by the contact angle). The PVDF/acid-MOF membrane showed the highest water flux of 558 LMH, resulting from its highest hydrophilicity due to the –OH functional groups.

The PEO solution was filtered through the PVDF, PVDF/MOF, and PVDF/acid-MOF membranes. The results of rejection are shown in Table 1. Although the PVDF/MOF and PVDF/acid-MOF membranes showed much higher water flux compared with the PVDF membranes, all the membranes maintained very similar rejection values. These results suggest that the pore sizes of the PVDF/MOF and PVDF/acid-MOF membranes were not changed by adding 0.25 wt% of MOF or acid-MOF particles [17]. Therefore, it is clear that the water flux through the modified PVDF membranes increased due to the larger macrovoids and the improved hydrophilicity.

Table 1
The rejection of PEO through PVDF, PVDF/MOF, and PVDF/acid-MOF membranes

Membranes	Rejection (%)
PVDF	84.74
PVDF/MOF	84.61
PVDF/acid-MOF	84.63

Table 2
Cu concentration in permeated water through PVDF, PVDF/MOF and PVDF/acid-MOF membranes (mean ± SD, $n = 3$)

Sample name	Cu conc. (unit: ppm)
D.I Water	0.01 ± 0.001
PVDF	0.001 ± 0.001
PVDF/MOF	0.041 ± 0.001
PVDF/acid-MOF	N.D.

To investigate the stability of the immobilized MOF and acid-MOF particles inside the PVDF membranes, the water that permeated through the membrane was collected for 1 h and analyzed by ICP-OES. The analytical results are shown in Table 2. The PVDF/MOF membranes suffered from Cu leaching, resulting in a Cu concentration that was 40 times higher compared to the virgin PVDF membrane. In contrast, the water that permeated through the PVDF/acid-MOF membrane showed no trace of Cu. Therefore, the addition of acid-MOF particles in the PVDF membrane shows potential for use in water permeation applications.

4. Conclusion

In this study, for the first time, hydrophilic MOF particles ($Cu_3(BTC)_2$ and acidified $Cu_3(BTC)_2$) were synthesized by the solvothermal method and dispersed in PVDF membranes for water treatment. Adding 0.25 wt% of MOF and acid-MOF particles to the PVDF membranes lowered their contact angle values from 79.8˚ (for the virgin PVDF membrane) to 69.2˚ and 64˚, respectively, indicating the improved hydrophilicity. In addition, the water fluxes of PVDF/MOF and PVDF/acid-MOF membranes were 299.7 and 558 LMH, respectively, which were 1.9 and 3.6 times higher than those of the pure PVDF membrane. Acid-MOFs were more stable and sufficiently immobilized in the PVDF membrane; no leaching of the metallic element was observed during water permeation. These results suggest the potential application of MOF particles as additives in polymer membranes for use in water treatment.

References

[1] F. Liu, N.A. Hashim, Y. Liu, M. Abed, K. Li, Progress in the production and modification of PVDF membranes, J. Membr. Sci. 375 (2011) 1–27.
[2] K. Jian, P.N. Pintauro, Asymmetric PVDF hollow-fiber membranes for organic/water pervaporation separations, J. Membr. Sci. 135 (1997) 41–53.
[3] D. Wang, K. Li, W. Teo, Preparation and characterization of polyvinylidene fluoride (PVDF) hollow fiber membranes, J. Membr. Sci. 163 (1999) 211–220.
[4] K. Yu Wang, T.-S. Chung, M. Gryta, Hydrophobic PVDF hollow fiber membranes with narrow pore size distribution and ultra-thin skin for the fresh water production through membrane distillation, Chem. Eng. Sci. 63 (2008) 2587–2594.
[5] A. Mansourizadeh, A. Ismail, T. Matsuura, Effect of operating conditions on the physical and chemical CO_2 absorption through the PVDF hollow fiber membrane contactor, J. Membr. Sci. 353 (2010) 192–200.
[6] S.J. Oh, N. Kim, Y.T. Lee, Preparation and characterization of PVDF/TiO_2 organic-inorganic composite membranes for fouling resistance improvement, J. Membr. Sci. 345 (2009) 13–20.
[7] F. Liu, M. Abed, K. Li, Preparation and characterization of poly(vinylidene fluoride) (PVDF) based ultrafiltration membranes using nano γ-Al_2O_3, J. Membr. Sci. 366 (2011) 97–103.
[8] A. Bottino, G. Capannelli, A. Comite, Preparation and characterization of novel porous PVDF-ZrO_2 composite membranes, Desalination 146 (2002) 35–40.
[9] L.Y. Yu, Z.L. Xu, H.M. Shen, H. Yang, Preparation and characterization of PVDF–SiO_2 composite hollow fiber UF membrane by sol–gel method, J. Membr. Sci. 337 (2009) 257–265.
[10] H. Li, M. Eddaoudi, M. O'Keeffe, O.M. Yaghi, Design and synthesis of an exceptionally stable and highly porous metal-organic framework, Nature 402 (1999) 276–279.
[11] T.H. Bae, J.S. Lee, W. Qiu, W.J. Koros, C.W. Jones, S. Nair, A high-performance gas-separation membrane containing submicrometer-sized metal-organic framework crystals, Angew. Chem. Int. Ed. 49 (2010) 9863–9866.
[12] B. Zornoza, A. Martinez-Joaristi, P. Serra-Crespo, C. Tellez, J. Coronas, J. Gascon, F. Kapteijn, Functionalized flexible MOFs as fillers in mixed matrix membranes for highly selective separation of CO_2 from CH_4 at elevated pressures, Chem. Commun. 47 (2011) 9522–9524.
[13] E.V. Perez, K.J. Balkus, J.P. Ferraris, I.H. Musselman, Mixed-matrix membranes containing MOF-5 for gas separations, J. Membr. Sci. 328 (2009) 165–173.
[14] S.F.E. Boerlage, M.D. Kennedy, M.R. Dickson, D.E.Y. El-Hodaliand, J.C. Schippers, The modified fouling index using ultrafiltration membranes (MFI-UF): Characterisation, filtration mechanisms and proposed reference membrane, J. Membr. Sci. 197 (2002) 1–21.
[15] S.F.E. Boerlage, M.D. Kennedy, M.R. Aniye, E. Abogrean, Z.S. Tarawneh, J.C. Schippers, The MFI-UF as a water quality test and monitor, J. Membr. Sci. 211 (2003) 271–289.
[16] V.V. Guerrero, Y. Yoo, M.C. McCarthy, H.K. Jeong, HKUST-1 membranes on porous supports using secondary growth, J. Mater. Chem. 20 (2010) 3938–3943.
[17] J.H. Choi, J. Jegal, W.N. Kim, Fabrication and characterization of multi-walled carbon nanotubes/polymer blend membranes, J. Membr. Sci. 284 (2006) 406–415.
[18] H.K. Kim, W.S. Yun, M.B. Kim, J.Y. Kim, Y.S. Bae, J. Lee, N.C. Jeong, A chemical route to activation of open metal sites in the copper-based metal-organic framework materials HKUST-1 and Cu-MOF-2, J. Am. Chem. Soc. 137(31) (2015) 10009–10015.

[19] M.H.P. Reddy, J.F. Pierson, S. Uthanna, Structural surface morphological, and optical properties of nanocrystalline Cu_2O and CuO films formed by RF magnetron sputtering: Oxygen partial pressure effect, Phys. Status Solidi A 209(7) (2012) 1279–1286.
[20] R.S. Kumar, S.S. Kumar, M.A. Kulandainathan, Efficient electrosynthesis of highly active $Cu_3(BTC)_2$-MOF and its catalytic application to chemical reduction, Microporous Mesoporous Mater. 168 (2013) 57–64.
[21] S. Takabayashi, T. Takahagi, Surface oxidation process of a diamond-like carbon film analyzed by difference X-ray photoelectron spectroscopy, Surf. Interface Anal. 47 (2015) 345–349.
[22] X. Jiang, N. Koizumi, X. Guo, C. Song, Bimetallic Pd–Cu catalysts for selective CO_2 hydrogenation to methanol, Appl. Catal. B 170–171 (2015) 173–185.
[23] D. Briggs, M.P. Seah (Eds.), Practical Surface Analysis, vol. 1, second ed., JohnWiley& Sons, New York, NY, 1993.
[24] E. Fontananova, J.C. Jansen, A. Cristiano, E. Curcio, E. Drioli, Effect of additives in the casting solution on the formation of PVDF membranes, Desalination 192 (2006) 190–197.
[25] J. Kong, K. Li, Oil removal from oil-in-water emulsions using PVDF membranes, Sep. Purif. Technol. 16 (1999) 83–93.
[26] X. Pan, L. Wang, Q. Zeng, L. Shi, R. Xu, J. Huang, K. Tang, Y. Xia, XPS study of polycrystalline diamond surfaces after annealing treatment, Surf. Coat. Technol. 228 (2013) S446–S448.
[27] C.P. Kealey, T.M. Klapötke, D.W. McComb, M.I. Robertson, J.M. Winfield, Fluorination of polycrystalline diamond films and powders. An investigation using FTIR spectroscopy, SEM, energy-filtered TEM, XPS and fluorine-18 radiotracer methods, J. Mater. Chem. 11 (2001) 879–886.
[28] J. Zhang, D. Jin, L. Zhao, X. Liu, J. Lian, G. Li, Z. Jiang, Preparation of nano-silver iodide powders and their efficiency as ice-nucleating agent in weather modification, Adv. Powder Technol. 22 (2011) 613–616.
[29] J. Kwon, S. Park, T.H. Lee, J.M. Yang, C.S. Lee, Investigation of oxidation inhibition properties of vaporized self-assembled multilayers on copper nanopowders, Appl. Surf. Sci. 257 (2011) 5115–5120.
[30] A. Roberts, D. Engelberg, Y. Liu, G.E. Thompson, M.R. Alexander, Imaging XPS investigation of the lateral distribution of copper inclusions at the abraded surface of 2024T3 aluminium alloy and adsorption of decyl phosphonic acid, Surf. Interface Anal. 33 (2002) 697–703.
[31] A. Ghahremaninezhad, D.G. Dixon, E. Asselin, Electrochemical and XPS analysis of chalcopyrite ($CuFeS_2$) dissolution in sulfuric acid solution, Electrochim. Acta 87 (2013) 97–112.